

Lymph Node Germinal Centers Form in the Absence of Follicular Dendritic Cell Networks

By Pandelakis A. Koni* and Richard A. Flavell*[§]

From the *Section of Immunobiology and [§]Howard Hughes Medical Institute, Yale University School of Medicine, New Haven, Connecticut 06520-8011

Summary

Follicular dendritic cell networks are said to be pivotal to both the formation of germinal centers (GCs) and their functions in generating antigen-specific antibody affinity maturation and B cell memory. We report that lymphotoxin β -deficient mice form GC cell clusters in the gross anatomical location expected of GCs, despite the complete absence of follicular dendritic cell networks. Furthermore, antigen-specific GC generation was at first relatively normal, but these GCs then rapidly regressed and GC-phase antibody affinity maturation was reduced. Lymphotoxin β -deficient mice also showed substantial B cell memory in their mesenteric lymph nodes. This memory antibody response was of relatively low affinity for antigen at week 4 after challenge, but by week 10 after challenge was comparable to wild-type, indicating that affinity maturation had failed in the GC phase but developed later.

Key words: lymphotoxin β • knockout mice • follicular dendritic cells • germinal centers • B cell memory

Follicular dendritic cells (FDCs)¹ are characterized by their location within B cell follicles and their extensive dendritic process networks, which retain antigen-Ig complexes via both complement receptors and Ig Fc receptors (for reviews, see references 1–4). Some antigen retained by FDCs is held within convolutions of the dendritic process network for periods of >1 yr and is thought to play an important role in the maintenance of long-term B cell memory. It is perhaps these same processes that have gained FDCs notoriety as a reservoir of HIV (5–8).

FDCs also give up some of their retained antigen much earlier, during the germinal center (GC) reaction. GCs are highly specialized structures that develop within primary B cell follicles upon antigenic challenge (9, 10). Antigen-specific B cells within GCs undergo somatic hypermutation of their antigen-binding receptor in a process of antibody affinity maturation (9–11). GC B cells are intimately associated with FDC dendritic processes, and antigen provided by FDC networks is thought to be critical for the selection of higher affinity clones within GCs and subsequent memory B cell formation (1–3, 12). FDCs also provide other soluble and contact-dependent signals which promote GC B cell viability, proliferation, and chemotactic responsiveness (4, 13). It has also been asserted that FDCs may be the

“nucleating force” for the initial formation of GCs within the specific anatomical location they occupy (4).

Lymphotoxin (LT) β is an immediate member of the TNF family, first identified by virtue of its ability to anchor LT α (TNF- β) to the surface of T cell hybridomas (14, 15). Both LT α and LT β are now known to be produced by activated B cells, activated T cells, and NK cells (16, 17). Effects of LT β R engagement include integrin upregulation (18), cytotoxicity (19, 20), and induction of chemokine production (21). Most notably, *lt α ^{-/-}* mice, *lt β ^{-/-}* mice, and *lt β r^{-/-}* mice lack peripheral LNs and Peyer’s patches, and have a disorganized splenic architecture with almost complete loss of GCs and FDC networks (22–29). Having said this, most *lt β ^{-/-}* mice still have mesenteric (M)LNs (26, 27, 30). Furthermore, the MLNs still form GC-like cell clusters in rudimentary B cell follicles despite the apparent lack of FDC networks (26, 30). Similar observations have been made in the spleen of *lt β ^{-/-}* mice and *lt β r^{-/-}* mice (27–29), although these studies also found residual FDC-like cells. Although not yet proven, the latter may be FDC precursors or immature FDCs but equally so might represent GC dendritic cells (GCDCs), which are distinct from FDCs and have so far been described in human tonsils (31) but not in mice.

Therefore, *lt β ^{-/-}* mouse MLNs appeared to present a unique model of in vivo GC reaction in the absence of FDC networks. Although other studies have suggested that GCs can form in the absence of antigen trapping on FDCs (32), an FDC-less mouse model was unprecedented and would further studies of GC reaction. *lt β ^{-/-}* mice might also facilitate the identification and evaluation of GCDCs. Finally, knowledge

¹Abbreviations used in this paper: APC, allophycocyanin; CG, chicken γ -globulin; DIG, digoxigenin; FDC, follicular dendritic cell; GC, germinal center; GCDC, GC dendritic cell; Lin, lineage; LT, lymphotoxin; MLN, mesenteric lymph node; NP, (4-hydroxy-3-nitrophenyl)acetyl; PNA, peanut agglutinin.

of the consequences of a lack of FDC networks will also be essential in assessing the potential utility of causing FDC regression. That is, it was recently reported that administration of soluble LT β R to adult mice results in temporary regression of FDC networks (33). Thus, there is now the prospect of being able to eliminate FDC networks in circumstances in which this might be considered likely to yield therapeutic benefit. For example, loss of FDC networks during triple drug therapy might eliminate this important HIV reservoir.

With all of this in mind, this study reports the dynamics of GC reaction and B cell memory formation in *lt β ^{-/-}* mice. Initiation of antigen-specific GCs in the MLNs of *lt β ^{-/-}* mice was relatively normal, but GC B cell numbers subsequently fell dramatically. GC B cells were clustered in the anatomical locations expected of GCs, indicating that this process is not critically dependent on FDC networks. *lt β ^{-/-}* mice also generated substantial B cell memory despite defective GC processes, albeit of relatively low affinity. Some antigen-specific antibody affinity maturation did occur and was even more apparent in the memory response, suggesting that somatic hypermutation had occurred. This is in agreement with other studies where somatic hypermutation was evident, even in the complete absence of GCs (24, 34).

Materials and Methods

Reagents. The protein G-Sepharose column-purified antibodies anti- λ 1 L chain (Ls136) and FDC-M2 were provided by Garnett Kelsoe (Duke University, Durham, NC) and Marie Kosco-Vilbois (Serono Pharmaceutical Research Institute, Geneva, Switzerland), respectively. Both were conjugated using a biotin coupling reagent (Boehringer Mannheim) at a biotin/antibody molar ratio of 10:1 and purified on a Sephadex G-25 column (Boehringer Mannheim). Rat anti-mouse IgD and anti-mouse CD11b (Mac-1) from PharMingen were also coupled as above but with digoxigenin (DIG) rather than biotin, also from Boehringer Mannheim.

Chicken γ -globulin (CG; Sigma) was conjugated with (4-hydroxy-3-nitrophenyl)acetyl (NP) succinimide ester (Calbiochem) in 0.1 M sodium borate, pH 9.2, to a NP/CG molar ratio of 13:1 (NP₁₃CG) and then dialyzed against PBS. PE (Molecular Probes) was haptenated in the same fashion but in the dark at a molar ratio of 20:1 to generate NP₂₀PE. BSA was also haptenated to create NP₂BSA and NP₁₅BSA. The precise degree of haptenation was not determined.

Animals and Animal Challenge. *Cd40l^{-/-}* mice and *lt β ^{-/-}* mice are those described previously (26, 35). Wild-type control mice were derived from original wild-type littermates of *lt β ^{-/-}* mice (26). *Ta α (β \times δ)^{-/-}* mice were generated from breeding pairs originally purchased from The Jackson Laboratory. All mice are on a mixed background of C57BL/6 and 129/Sv and were housed in specific pathogen-free conditions. All experiments were conducted in accordance with Yale University Animal Care and Use guidelines.

Mice at 6–8 wk of age were challenged intraperitoneally with 50 μ g of either CG or NP₁₃CG, both of which were adsorbed to alum in 0.1 ml PBS. Some mice at various times may have received a second challenge of 200 μ g NP₁₃CG in 0.1 ml PBS alone.

Hyperimmunized mouse serum for the purpose of anti-NP antibody standardization (see below) was obtained from wild-type mice 6 d after being boosted with 0.2 mg NP₁₃CG in PBS, 27 d after the primary challenge with 50 μ g NP₁₃CG adsorbed to alum.

MLN Histology. MLNs were frozen in Tissue-Tek OCT

compound (VWR Scientific) using a dry-ice/methylbutane bath and stored at -70°C until cutting. Sections of 5- μm thickness were cut onto silanized glass slides, fixed in cold acetone for 10 min, air-dried, and then stored at -70°C until use. For staining, sections were thawed for 30 min and then rehydrated in PBS for 20 min. Endogenous peroxidase was quenched with 0.3% hydrogen peroxide for 5 min. Sections were washed in PBS for 10 min and then preblocked with PBS/3% BSA/0.1% Tween 20 for 30 min in a humidified chamber. Staining for IgD was with rat anti-IgD (Southern Biotechnology Associates) and then horseradish peroxidase-conjugated goat anti-rat IgG (Southern Biotechnology Associates). The presence of FDCs was assessed with biotin-conjugated FDC-M2 (see Reagents). Other biotin-conjugated antibodies were anti-CD23 and anti-CD24, both from PharMingen. All biotin conjugates used a secondary step of alkaline phosphatase-conjugated streptavidin (Zymed). Incubations were in a humidified chamber for 1 h. Washes between steps were with PBS/0.1% Tween 20. Substrates for horseradish peroxidase and alkaline phosphatase were diaminobenzidine (brown) and NBT/BCIP (purple-blue), respectively (Zymed). Counter-staining was with nuclear fast red (Zymed).

MLN Cell Preparation. MLNs were harvested into 0.5 ml cold digest buffer in a 4-well plate (Nunc) on ice. Digest buffer was Bruff's medium with 5% FCS, 0.1 mg/ml collagenase type IV (Sigma), and 0.1 mg/ml deoxyribonuclease type I (Sigma). Bruff's medium is Click's medium (Irvine Scientific) supplemented with 40 mM l-glutamine, 60 μM 2-ME, 0.7 mM sodium bicarbonate, and 58 mg/l gentamycin. The capsule of each MLN was torn and teased open with 27-gauge needles before incubating plates at 37°C for 30 min. Capsules were then further disrupted to release MLN cells by pipetting. The cell suspension was made up to 10 ml with Bruff's/5% FCS, filtered through 0.1-mm nylon mesh (Small Parts, Inc.), and centrifuged at 800 revolutions/min in a bench-top centrifuge at 4°C for 5 min. Finally, cells were resuspended in 2 ml Bruff's/5% FCS for fluorocytometry or antigen-specific antibody determination as described below.

Fluorocytometry. MLN cells were prepared as described above, and aliquots of 10^6 cells were resuspended into 0.2 ml PBS/1% FCS supplemented with 5 $\mu\text{g/ml}$ FcBlock (PharMingen). Samples were left on ice for 30 min before primary antibodies were added, and were then left on ice in the dark for an additional 1 h. Samples were washed by being made up to 1.2 ml with PBS/1% FCS before centrifugation at 800 revolutions/min at 4°C for 5 min. Secondary antibody incubation and rewashing were done as above. Four-color fluorocytometry used a FACSCalibur[®] with argon and helium-neon lasers (Becton Dickinson). Data from 2.5×10^5 events were analyzed with CellQuest software by first gating on lymphocytes/lymphoblasts, based on forward and side scatter. PharMingen antibodies used included anti-CD4-allophycocyanin (APC; L3T4, RM4-5), anti-CD8 α -APC (53-6.7), anti-CD90.2-APC (53-2.1), GL7-FITC, anti-CD45R-FITC, anti-CD24-biotin (M1/69), and anti-CD45R-biotin. Peanut agglutinin (PNA)-biotin, streptavidin-Cy-Chrome, and anti-digoxin-Cy5 were from Vector, PharMingen, and Jackson Laboratories, respectively. Other reagents used were anti- λ 1-biotin, anti-IgD-DIG, and anti-CD11b-DIG, described in Reagents above.

MLN Antigen-specific Antibody Determination. Antigen-specific antibody determination was done essentially as described by Kelly et al. (36), using antibody-secreting cells directly in an ELISA. Maxisorp 96-well plates (Nunc) were coated at 4°C for 16–20 h with 10 $\mu\text{g/ml}$ NP₂BSA or NP₁₅BSA in PBS, 0.1 ml aliquot per well. Plates were then washed four times with PBS before blocking with PBS/1% FCS for 2–3 h. Meanwhile, MLN

cells were prepared at 10^7 cells per ml of Bruff's/5% FCS as described above. MLN cell aliquots of 0.1 ml were then plated in wells and cultured at 37°C for 5 h alongside a twofold serial dilution of serum from a standard hyperimmunized wild-type mouse (see above; serum dilution was with PBS/1% FCS). Subsequent washes were with PBS/0.05% Tween 20. Ig detection used isotype-specific alkaline phosphatase-conjugated reagents and pNPP substrate as described (Southern Biotechnology Associates). OD_{405} was determined with a microplate reader (model 550; BioRad). Typically, a 1:12,800 dilution of hyperimmunized wild-type mouse serum gave an OD_{405} of ~ 2.7 and 1.9 above background for IgG1 detected with NP_2BSA and NP_{15}BSA , respectively. The lower limit of detection was typically at a serum dilution of 1:1,638,400, giving an OD_{405} of ~ 0.05 –0.10 above background. The anti-NP-specific antibody titer of samples was expressed as relative units, representing the reciprocal of the standard serum dilution giving the same OD_{405} as the sample. Calculations were by four-parameter analysis using Microplate Manager III software (BioRad).

Serum Antigen-specific Antibody Determination. Blood was harvested from mice for serum by cardiac puncture at the time of culling. Maxisorp plates were coated with NP_2BSA or NP_{15}BSA , blocked, and washed as described above. Serum aliquots of 0.1 ml ($1:10^5$ in PBS/1% FCS) were applied to wells for 1 h alongside a twofold serial dilution of serum from a hyperimmunized wild-

type mouse (see above; serum dilution was with PBS/1% FCS). Antigen-specific Ig determination then proceeded as described in the previous section.

Results

Lt $\beta^{-/-}$ Mice Form GC B Cell Clusters but Lack FDCs. We showed previously that *lt $\beta^{-/-}$* mice form PNA-binding, $\text{IgD}^- \text{B220}^+$ cell clusters in B cell areas of their MLNs (26, 30), characteristic of GCs (37). Although IgD^+ B cells were also found to infiltrate T cell areas, the GC-like B cell clusters were within IgD^+ B cell follicles at the periphery of MLNs, as in wild-type mouse MLNs (26, 30). These observations were extended here by staining for CD24. Primary follicle B cells are CD24^+ , but GC B cells are CD24^{hi} (38–40; Fig. 1 A). This also appeared to be true of *lt $\beta^{-/-}$* GC B cell clusters (Fig. 1 B). Again, the *lt $\beta^{-/-}$* GC B cells were clustered within the location expected of wild-type GCs.

Immunohistology with anti-complement receptor 1 (CR-1) and FDC-M1 suggested that *lt $\beta^{-/-}$* mice lack FDCs (26). We subsequently showed that although wild-type mouse MLNs have very large amounts of IgM immune complex

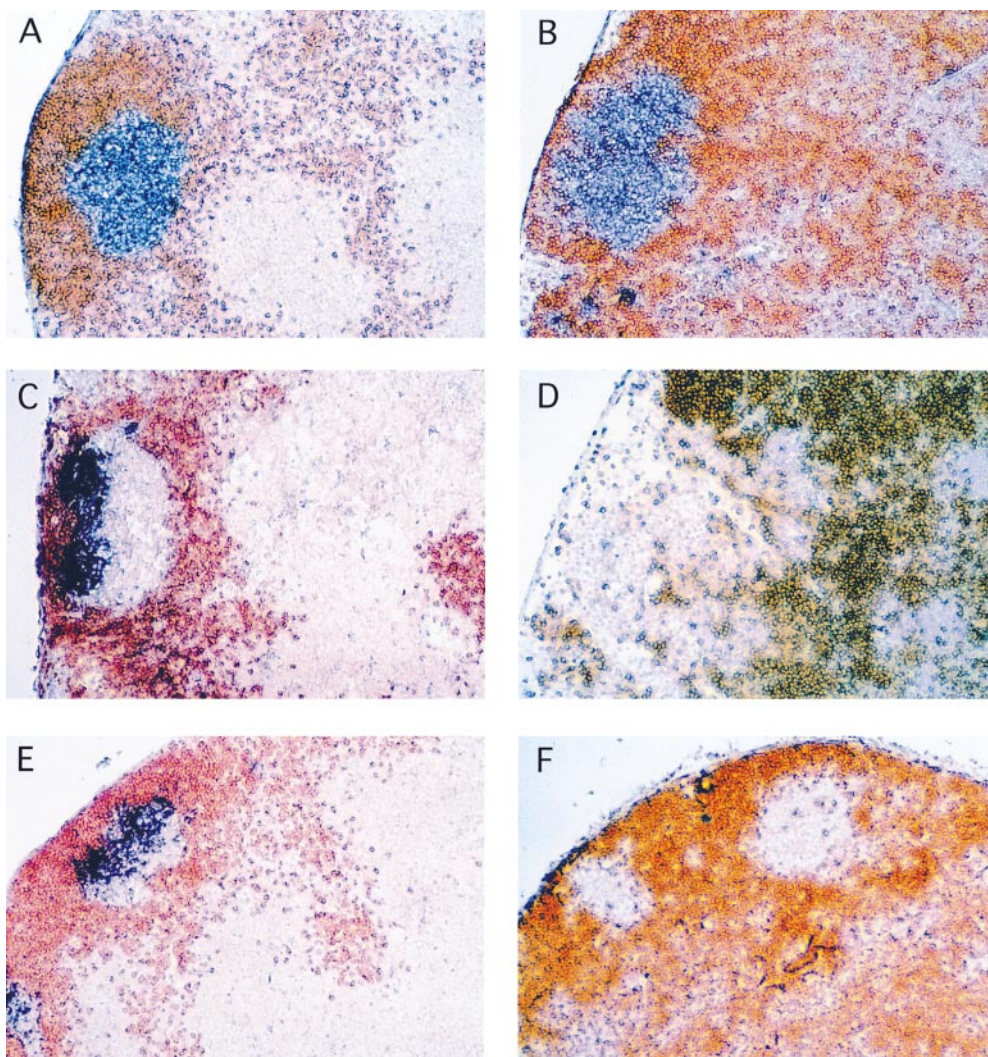


Figure 1. *Lt $\beta^{-/-}$* mice generate GC B cell clusters without FDCs. MLNs were from unchallenged 6–8-wk-old wild-type mice (A, C, and E) and *lt $\beta^{-/-}$* mice (B, D, and F) and show GCs generated at random times as a result of environmental antigens. Staining for IgD in all panels is brown. CD24 (A and B), CD23 (C and D), and FDC-M2 (E and F) are purple-blue. The intensely colored cells in D (*lt $\beta^{-/-}$*) are B cells, which are both IgD^+ and CD23^+ . This intense color is not as strong in C (wild-type), presumably because the intensely CD23^{hi} FDCs have “quenched” the color reaction somewhat. Fluorocytometry did not reveal any significant difference in CD23 levels between wild-type and *lt $\beta^{-/-}$* MLN cells (data not shown). Original magnification: $\times 62.5$.

on FDCs, $lt\beta^{-/-}$ mouse MLNs did not have any such deposits (30). However, despite all of the above, it is possible that Ig Fc receptor-bearing (FcR^+) FDCs (3, 4, 9) constitute a distinct subset of FDCs which are negative for both FDC-M1 and CR-1. It is also conceivable that antigen-Ig complexes retained on such FcR^+ FDCs may support GC reaction in the absence of CR-1⁺ FDCs. In potential support of this, mice deficient in CR-1 still possess GCs (41, 42), albeit somewhat smaller than wild-type.

Therefore, an evaluation was made as to whether or not $lt\beta^{-/-}$ mice possess FcR^+ FDC networks by staining for CD23 (43). This revealed that $lt\beta^{-/-}$ mice completely lack FcR^+ FDC networks (Fig. 1 D), and that the $lt\beta^{-/-}$ GC B cell clusters were CD23⁻ compared with the surrounding follicle B cells, as expected of wild-type GC B cells (9; Fig. 1 C). FDC networks clearly stained very strongly for CD23 in wild-type mouse MLNs (Fig. 1 C), and were observed in every B cell follicle regardless of whether or not there was an ongoing GC reaction. Some discrete CD23^{lo} cells were seen in the $lt\beta^{-/-}$ mouse MLN CD23-IgD⁻ GC cell clusters (Fig. 1 D). These cells most likely represent GC B cells that have not yet fully downregulated CD23, but it is conceivable that they represent immature FDCs or the mouse equivalent of GCDCs (31).

Finally, the lack of staining by FDC-M2 further emphasized the complete absence of FDC networks in the MLNs of $lt\beta^{-/-}$ mice (Fig. 1 F). Although FDC-M2 has not been fully characterized, it is a useful marker of FDC networks (Fig. 1 E). Like CD23, FDC-M2 staining was observed in every wild-type mouse MLN B cell follicle regardless of whether or not there was an ongoing GC reaction (data not shown). As with CD23, a low level of FDC-M2 staining may well mark immature FDCs or another cell type such as the mouse equivalent of GCDCs (31). Neither immature FDCs nor mouse GCDCs have yet been defined.

$lt\beta^{-/-}$ Mice Show Increased GC B Cells upon Intraperitoneal Challenge. Four-color flow cytometry was adopted in order to study further the GC reaction in $lt\beta^{-/-}$ mouse MLNs (see Materials and Methods). Most non-GC B cells were excluded as "lineage"-positive (Lin^+) cells, using a combination of antibodies against CD4, CD8 α , CD90.2,

IgD, and CD11b (Fig. 2). Markers to discriminate GC B cells included PNA binding (37, 38), anti-CD24 (38–40), and GL7 (44). PNA binding and CD24 are increased on GC B cells, whereas GL7 recognizes an activation antigen found on GC B cells but not naive or memory B cells. Fluorescence cytometry of MLNs is simple compared with spleen due to the relative lack of immature B cells, granuloid cells, and erythroid cells. After excluding nonlymphoid particles of low forward scatter (data not shown), most Lin^- cells in MLNs are PNA^{hi}CD24^{hi} (data not shown). This is demonstrated in Fig. 2 with MLNs 12 d after intraperitoneal challenge with CG adsorbed to alum.

As expected, both T cell-less mice and $cd40l^{-/-}$ mice fail to generate GC B cells (Fig. 2), most clearly demonstrated with GL7. Both wild-type mice and $lt\beta^{-/-}$ mice revealed substantial levels of Lin^-GL7^+ cells in their MLNs, although $lt\beta^{-/-}$ mice consistently had lower levels than wild-type mice (see also below). Lin^-GL7^+ cells represented about half of all $Lin^-PNA^hiCD24^hi$ cells (Fig. 2) and were CD45R⁺ (data not shown; see below). Lin^- cells include non-GC B cells such as antibody-secreting cells and memory B cells, which would be GL7⁻.

The levels of Lin^-GL7^+ GC B cells at day 12 after challenge (Fig. 2) were much higher than those in unchallenged mice, and were similar to those observed in the spleen with the same antigenic challenge (45). Without intraperitoneal challenge, the levels of Lin^-GL7^+ cells were 0.3–0.7% of total MLN cells in both wild-type mice and $lt\beta^{-/-}$ mice (data not shown; see below), consistent with levels in the spleen of unchallenged wild-type mice (45). Thus, intraperitoneal challenge in alum is an effective means of inducing GC B cell generation in the MLNs of both wild-type mice and $lt\beta^{-/-}$ mice.

$lt\beta^{-/-}$ Mice Generate Antigen-specific GC B Cells. The hapten NP has been used extensively in GC studies (40, 45–48). The primary response to NP is dominated by antibodies bearing a $\lambda 1$ light chain, recognized by the antiidiotype antibody Ls136 (39, 49–52). NP-specific antibody-bearing cells can also be followed by their capacity to bind NP-conjugated PE (NP₂₀PE). NP also provides a means for evaluating anti-NP-specific antibody affinity maturation (described below).

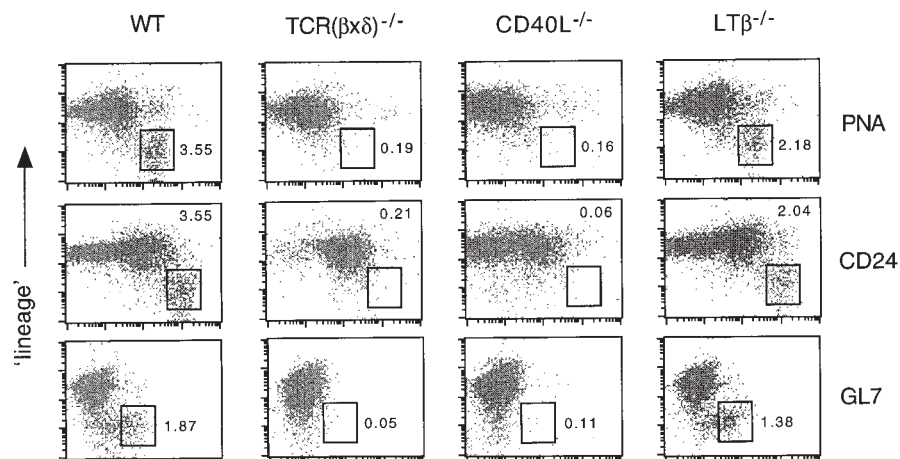


Figure 2. Fluorescence cytometry reveals GC B cells in $lt\beta^{-/-}$ mouse MLNs. Most non-GC B cells were excluded as Lin^+ cells (see text). GC B cells were further identified with PNA, CD24, and GL7. Plots shown are a representative experiment using MLN 12 d after intraperitoneal challenge with 50 μ g CG adsorbed to alum. The boxed areas include GC B cells, and the numbers alongside them indicate the percentage of the total MLN cells therein. WT, wild-type.

Mice were challenged intraperitoneally with either CG or NP-haptenated CG (NP₁₃CG), and MLNs were examined for NP-specific response 8 d later. Both wild-type mice and *ltβ*^{-/-} mice showed massive numbers of λ1⁺ NP₂₀PE-binding MLN cells in response to NP₁₃CG (Fig. 3). The percentage of CD45R⁺ cells that were λ1⁺ NP₂₀PE-binding were 66.1 ± 18.2 and 76.6 ± 17.2 for wild-type mouse MLNs and *ltβ*^{-/-} mouse MLNs, respectively (*n* = 6 each), compared with <0.1% in unchallenged mice. As expected (46), CG itself did not elicit any significant levels of λ1⁺ NP₂₀PE-binding cells (data not shown). Also, T cell-less mice and *cd40l*^{-/-} mice did not show significant levels of λ1⁺ NP₂₀PE-binding cells (Fig. 3).

NP-specific GC B cells were also evident in MLNs from both wild-type mice and *ltβ*^{-/-} mice at day 8 after challenge (Fig. 4), defined as the Lin⁻GL7⁺ subset (see Fig. 2). Both the fraction of *ltβ*^{-/-} GC B cells that were NP₂₀PE-binding and the intensity of NP₂₀PE-binding appeared to be relatively normal (Fig. 4). The response of wild-type mice and *ltβ*^{-/-} mice was then followed from day 8 to day 24 after challenge (Fig. 5). As early as day 12 after challenge, *ltβ*^{-/-} mouse MLN λ1⁺ GC B cells were greatly reduced compared with wild-type, and even fewer were NP₂₀PE-binders (Fig. 5). Having said this, the rate of decline of *ltβ*^{-/-} GC B cells was not sustained at day 16 after challenge. Instead, Lin⁻GL7⁺λ1⁺ *ltβ*^{-/-} GC B cell levels appeared to plateau such that they were comparable to wild-type at day 20 after challenge before then falling again by day 24 (Fig. 5). This pattern was reflected among Lin⁻GL7⁻λ1⁺ non-GC cells.

***ltβ*^{-/-} Mice Generate Antigen-specific Memory B Cells.** Both *ltβ*^{-/-} mice and wild-type mice showed anti-NP antibody secretion among MLN cells at day 6 after challenge with 50 μg NP₁₃CG adsorbed to alum (Fig. 6). IgA and IgG2a were not detected at all (data not shown). Clearly, IgG1 secretion by *ltβ*^{-/-} mouse MLN cells (average relative units = 0.91) was much lower than wild-type (average = 6.03), perhaps indicating a lack of T cell and/or dendritic cell help. Nonetheless, this level of IgG1 secretion by *ltβ*^{-/-} mouse MLNs was ~20-fold higher than the lower limit of detection. Also, a primary challenge with 0.2 mg NP₁₃CG in PBS alone did not result in significant anti-NP antibody secretion by either wild-type or *ltβ*^{-/-} mouse MLN cells at day 6 after challenge (data not shown). Thus, the response to NP₁₃CG in PBS was a good indicator of memory generated as a result of primary challenge with NP₁₃CG adsorbed to alum (see below).

To determine whether or not humoral memory was generated, mice were challenged as before and then rechallenged at various times with either 0.2 mg NP₁₃CG in PBS

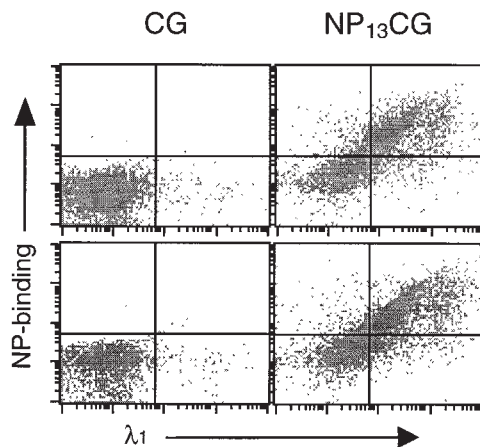


Figure 4. *ltβ*^{-/-} mice generate antigen-specific GC B cells. Plots show NP₂₀PE-binding and surface λ1 antibody chain among Lin⁻GL7⁺ GC B cells from wild-type mouse MLNs (top) and *ltβ*^{-/-} mouse MLNs (bottom) at day 8 after challenge with 50 μg NP₁₃CG adsorbed to alum.

without alum or PBS alone. 6 d later, anti-NP antibody was determined among MLN cells and in serum. Both the level of anti-NP antibody and the relative affinity for NP were determined by ELISA using two different BSA substrates. Total and relatively high affinity anti-NP antibody were determined with densely (NP₁₅BSA) and sparsely (NP₂BSA) haptenated BSA, respectively. As GC reaction proceeds, a greater proportion of anti-NP antibody becomes detectable with NP₂BSA. The principal of this approach has been used in several other studies (24, 26, 34), and was recently validated with mAbs of various affinity for NP (45).

When given a secondary challenge and harvested at week 4, *ltβ*^{-/-} mouse MLNs appeared to secrete more anti-NP antibody than wild-type mouse MLNs (Fig. 7), implying that *ltβ*^{-/-} mice had generated greater humoral memory than wild-type mice. This pattern was not so apparent in serum (Fig. 7). Nonetheless, *ltβ*^{-/-} mice clearly showed memory even in their serum. The substantial memory response was still evident among *ltβ*^{-/-} mouse MLNs at week 10 after challenge but was less evident in serum (Fig. 7).

Both wild-type mouse MLNs and *ltβ*^{-/-} mouse MLNs showed affinity maturation in the post-GC phase between weeks 4 and 10 after challenge (Fig. 7). Thus, the relatively low NP₂/NP₁₅ ratio in *ltβ*^{-/-} mouse MLNs at week 4 after challenge was almost normal at week 10. Again, this observation in MLNs was not obvious in serum (Fig. 7). At both weeks 4 and 10 after challenge, *ltβ*^{-/-} mice showed a lower NP₂/NP₁₅ ratio in their serum than wild-type mice, indicating a defect in GC affinity maturation processes.

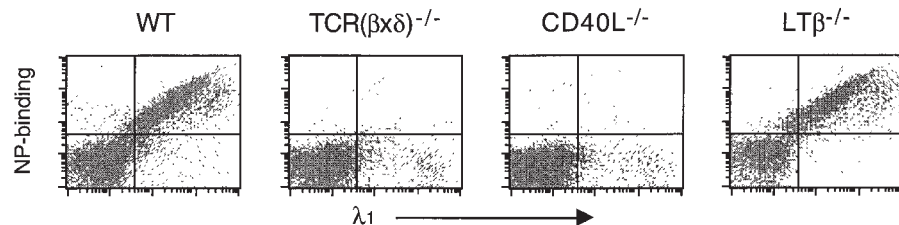


Figure 3. *ltβ*^{-/-} mice show antigen-specific B cell expansion in their MLNs. MLNs were harvested at day 8 after challenge with 50 μg NP₁₃CG adsorbed to alum, and cells were examined for NP₂₀PE-binding and surface λ1 antibody chain. WT, wild-type.

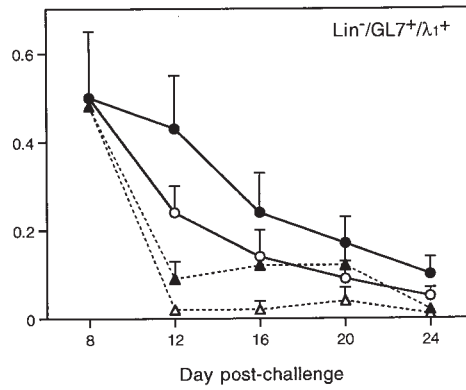
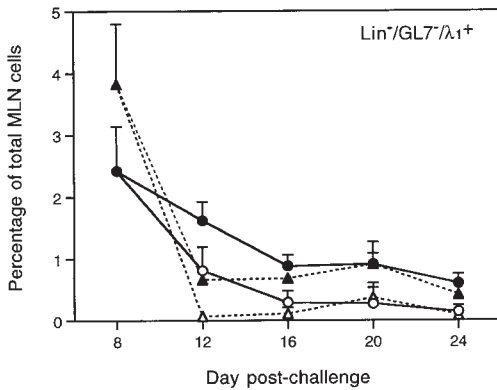


Figure 5. *Ltβ*^{-/-} GC and non-GC antigen-specific MLN cells decline rapidly. MLNs were harvested at various times after challenge with 50 μg NP₁₃CG adsorbed to alum. Antigen-specific GC and non-GC cells were defined as Lin⁻GL7⁺λ1⁺ and Lin⁻GL7⁻λ1⁺ cells, respectively. Wild-type mouse MLN cells (circles) and *ltβ*^{-/-} mouse MLN cells (triangles) are shown as both total Lin⁻λ1⁺ cells (filled symbols) and as cells therein that also bound NP₂₀PE (open symbols). 4–6 mice were used per group and are represented as the average plus SD (8 of 38 *ltβ*^{-/-} mice used for this study did not appear to have MLNs).

Discussion

Numerous lines of evidence have now shown that *ltβ*^{-/-} mice do not have FDC networks (26, 27, 30, and this study). In addition, MacKay and Browning (33) have very recently shown that administration of soluble LTβR to adult mice causes regression of FDC networks and dissipation of the antigen they were retaining. Clearly however, *ltβ*^{-/-} mice might still have FDC precursors. Indeed, irradiated adult *ltα*^{-/-} mice generate mature FDC networks of *ltα*^{-/-} origin upon reconstitution with wild-type bone marrow (53), and equivalent results have been obtained with *ltβ*^{-/-} mice (data not shown). The location of FDC precursors in *ltβ*^{-/-} mice is at present unknown, and it is conceivable that they will be found within B cell follicles and GCs even though they fail to develop into mature FDC networks. Others have shown that *ltβ*^{-/-} mice and *ltβr*^{-/-} mice do have small numbers of discrete FDC-M2⁺ cells in the spleen (27, 28), leading to the suggestion that these cells may represent FDC precursors or immature FDCs. However, there is no evidence that FDC-M2 is com-

pletely specific for FDCs, although it is a useful marker of FDC networks. Unlike FDC-M2, FDC-M1 has been well characterized and is considered to be relatively FDC specific, but even this marker also stains tingible body macrophages (which are found in GCs) and some endothelial cells (54).

The origin of FDCs is somewhat controversial (for a review, see reference 55) and will undoubtedly be further complicated by the fact that mice may also prove to have GCDCs (31), which might be the FDC-M2⁺ cells seen by others. Regardless of whether or not *ltβ*^{-/-} mice have FDC precursors, the roles FDCs are said to fulfill largely rely on the extensive dendritic processes of FDC networks. Clearly, these structures are absent.

The absence of FDC networks presumably has indirect as well as direct effects on GC reactions. For example, this study has not considered GC T cells in *ltβ*^{-/-} mice. Other defects clearly exist in *ltβ*^{-/-} mouse MLNs, such as the B cell infiltration of the T cell areas and reduced primary humoral response. What this study has attempted to do is highlight the processes that occur despite the defects. Most notably, *ltβ*^{-/-} mice generate antigen-specific GC B cells and class-switched memory B cell responses. Having said this, antigen-specific *ltβ*^{-/-} GC B cells decline rapidly at times when wild-type GC B cell numbers are still relatively high. GCs normally have a life span of a few weeks (10, 56). It has been argued that the regression of GCs begins at a time when FDCs begin to bury their retained antigen within membrane pockets, thereby ceasing to present antigen to GC B cells (56). The decline of *ltβ*^{-/-} GC B cells in the absence of FDC networks may be a premature execution of this process. On the other hand, *ltβ*^{-/-} GC B cell numbers did not decline further between days 12 and 16 after challenge but instead appeared to plateau until they finally decreased further between days 20 and 24. It is conceivable that the Lin⁻GL7⁺λ1⁺ cell numbers were maintained by further generation of such cells from centroblasts.

Anti-NP memory and relative affinity maturation were assessed at various times. The humoral memory response in *ltβ*^{-/-} mouse MLNs was as great if not greater than that seen in wild-type mouse MLNs (Fig. 7). Of course, this

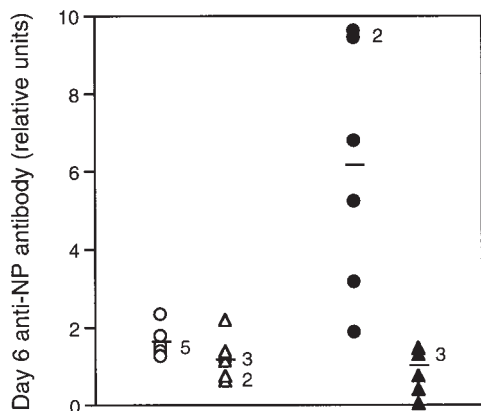


Figure 6. *Ltβ*^{-/-} mice generate reduced but significant antigen-specific antibody in their MLNs. MLNs were harvested from six wild-type mice (circles) and *ltβ*^{-/-} mice (triangles) at day 6 after challenge with 50 μg NP₁₃CG adsorbed to alum and were assayed for IgM (open symbols) and IgG1 (filled symbols) using NP₁₅BSA as the detection substrate. Data are shown as relative units using IgG1 detection in the serum of a hyperimmunized wild-type mouse as a standard (see Materials and Methods).

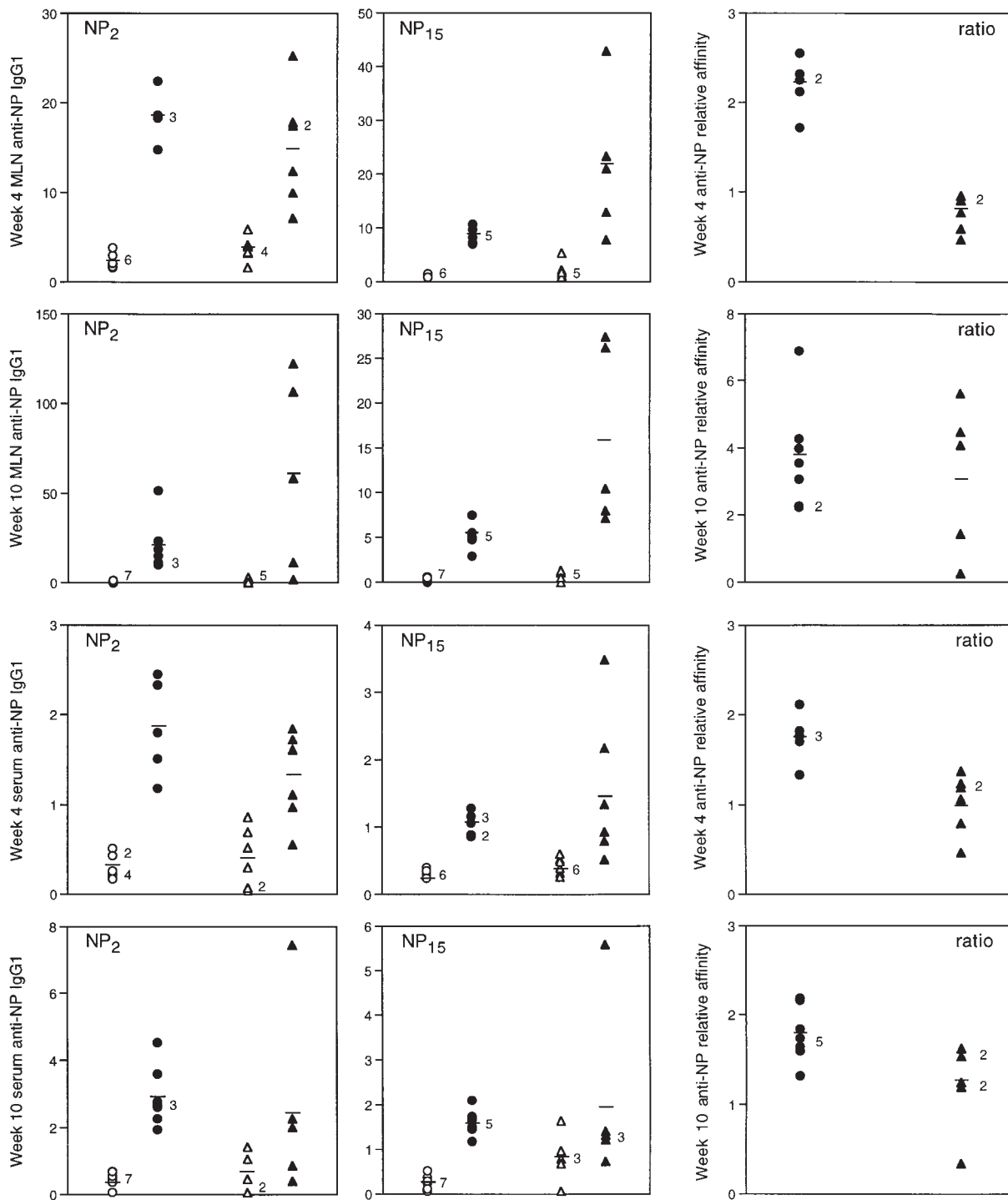


Figure 7. *Ltβ^{-/-}* mice generate humoral memory and show post-GC affinity maturation. Mice were harvested at both week 4 and week 10 after challenge with 50 μg NP₁₃CG adsorbed to alum. Anti-NP antibody levels were followed in MLNs (top two rows) and serum (bottom two rows) using five to seven wild-type mice (circles) and *Ltβ^{-/-}* mice (triangles) per group. Some groups were given a secondary challenge of 0.2 mg NP₁₃CG in PBS alone 6 d before culling (filled symbols), while others were given just PBS (open symbols). Data are shown for both NP₂BSA and NP₁₅BSA as detection substrate (8 of 32 *Ltβ^{-/-}* mice used for this study did not appear to have MLNs). Anti-NP IgG1 relative units ($\times 10^{-5}$) represent the reciprocal of the standard serum dilution giving the same OD₄₀₅ as the sample. Note that the MLN anti-NP IgG1 assays are not directly comparable with the serum assays. Also shown are the resultant NP₂/NP₁₅ ratios of the memory responses (filled symbols), which are a reflection of relative anti-NP affinity. Numbers alongside various data points indicate overlapping mice, and bars represent averages.

may not be a direct reflection of the actual frequency of NP-specific memory B cells. The relatively low level of NP-specific non-GC B cells ($\text{Lin}^{-}\lambda 1^{+}$ NP₂₀PE-binding) in $It\beta^{-/-}$ mouse MLNs late in the GC phase (Fig. 5) suggests that $It\beta^{-/-}$ mouse MLNs produce significantly fewer memory B cells than wild-type mouse MLNs.

The degree of affinity maturation observed in serum here was similar to that previously reported for $It\alpha^{-/-}$ mice, Lyn kinase ($lyn^{-/-}$) mice, and $It\beta^{-/-}$ mice (24, 26, 34). Affinity maturation requires somatic hypermutation and subsequent selection of higher affinity clones, suggesting that specific activated B cells had entered into a "GC B cell program" despite the complete absence of GCs in $It\alpha^{-/-}$ mice and $lyn^{-/-}$ mice. Indeed, somatic hypermutation is evident in $It\alpha^{-/-}$ mice and $lyn^{-/-}$ mice (24, 34), and there is no reason to believe that this is not occurring in $It\beta^{-/-}$ mice. Certainly, somatic hypermutation is normally evident as early as day 7 after challenge (40, 45, 48, 57, 58) and, unlike $It\alpha^{-/-}$ mice (24) and $lyn^{-/-}$ mice (34), $It\beta^{-/-}$ mice generate appreciable levels of antigen-specific GC B cells upon challenge (this study).

Where and how are high-affinity mutants selected in the absence of GCs? Takahashi et al. (45) recently described evidence in support of a phenomenon best described as "post-GC intraclonal competition." The average affinity of anti-NP antibody from bone marrow antibody-secreting cells continued to increase long after the GC reaction had waned (45). Although clonal selection occurs independently in each GC and low-affinity B cells can survive the selection process within GCs if high-affinity competitors are absent (45), post-GC affinity-driven selection processes effectively constitute "inter-GC selection." This concept is supported by the study here, where the relative affinity of anti-NP antibody at week 10 after challenge was about twofold higher than that at week 4 after challenge (Fig. 7), in the MLNs of wild-type mice and $It\beta^{-/-}$ mice.

Thus, mutants with higher affinity for the antigen are generated and selected even in $It\beta^{-/-}$ mice, but the highest possible affinity for antigen is not achieved in $It\beta^{-/-}$ mice (Fig. 7), presumably because further rounds of somatic mutation cannot occur in the post-GC phase. Hence, despite post-GC intraclonal competition, the benefit of the GCs is as an environment in which repeated rounds of somatic mutation and selection can occur rapidly in order to achieve the highest possible affinity for antigen. Indeed, al-

though substantial somatic hypermutation was observed in $It\alpha^{-/-}$ mice, the degree of mutation among V186.2 genes was only about half that seen in wild-type mice (24).

It should also be borne in mind that the apparent degree of affinity maturation by post-GC intraclonal competition will vary substantially depending on the nature of the antigen. In some experimental instances, random mutations lead to higher affinity clones at a relatively high frequency (59). The NP hapten used here and by others (24, 34, 45) would appear to be another such example, since a frequently occurring single point mutation in the V186.2 gene (24, 60) is associated with greatly increased affinity for NP (61). Thus, the studies here showing defective NP-specific affinity maturation in $It\beta^{-/-}$ mice can only be interpreted to suggest that affinity maturation within GCs has failed in these mice.

Recirculating memory B cells migrate between secondary lymphoid organ follicles where they can respond to antigen held on FDC networks (62, 63). Marginal zone memory B cells are said to be long-lived and non-recirculating (64–66), and it is difficult to conceive of how their maintenance could be dependent on antigen retained by FDC networks. As the name suggests, marginal zone memory B cells have been best characterized in the marginal zone of the spleen, where they are seen to appear both immediately before and during GC reactions (63–65). Equivalent areas are located on the inner wall of the subcapsular sinus of LNs, and may be substantial in MLNs (65). Further studies will be necessary to characterize the B cell memory in $It\beta^{-/-}$ mice, including how the nature and dose of antigen might affect memory maintenance besides memory generation per se.

In conclusion, this study has considered GC reactions in the MLNs of $It\beta^{-/-}$ mice and found that both GC and B cell memory are formed despite the complete absence of FDC networks. However, antigen-specific antibody affinity maturation is defective. This study of the MLNs of $It\beta^{-/-}$ mice serves as a model for the consequences of administration of soluble LT β R with respect to LNs. The spleen of $It\beta^{-/-}$ mice was not studied here because it is more disorganized than the MLNs (26, 27, 30). The fact that anti-NP memory at week 10 was much less apparent in serum than in MLNs (Fig. 7) may well be a reflection of the fact that serum antibody levels are dominated by the spleen and spleen-derived bone marrow antibody-secreting cells. Having said this, even the spleen of $It\beta^{-/-}$ mice generates some PNA-binding GC-like B cells (27).

We are indebted to Garnett Kelsoe for Ls136 antibody, Marie Kosco-Vilbois for FDC-M2 antibody, Frank Wilson for technical assistance, Fran Manzo for clerical assistance, and Michiko Shimoda for invaluable advice and discussion.

This study was supported by the American Diabetes Association and the Howard Hughes Medical Institute. R.A. Flavell is an Investigator of the Howard Hughes Medical Institute.

Address correspondence to Richard A. Flavell, Section of Immunobiology and Howard Hughes Medical Institute, 310 Cedar St., FMB412, Yale University School of Medicine, New Haven, CT 06520-8011. Phone: 203-737-2216; Fax: 203-785-7561; E-mail: richard.flavell@qm.yale.edu

Received for publication 1 December 1998 and in revised form 15 January 1999.

References

1. Klaus, G.G.B., J.H. Humphrey, A. Kunkl, and D.W. Dongworth. 1980. The follicular dendritic cell: its role in antigen presentation in the generation of immunological memory. *Immunol. Rev.* 53:3–28.
2. Mandel, T.E., R.P. Phipps, A. Abbot, and J.G. Tew. 1980. The follicular dendritic cell: long term antigen retention during immunity. *Immunol. Rev.* 53:29–59.
3. Schriever, F., and L.M. Nadler. 1992. The central role of follicular dendritic cells in lymphoid tissues. *Adv. Immunol.* 51:243–284.
4. Tew, J.G., J. Wu, D. Qin, S. Helm, G.F. Burton, and A.K. Szakal. 1997. Follicular dendritic cells and presentation of antigen and costimulatory signals to B cells. *Immunol. Rev.* 156:39–52.
5. Schragar, L.K., and A.S. Fauci. 1995. Trapped but still dangerous. *Nature.* 377:680–681.
6. Heath, S.L., J.G. Tew, J.G. Tew, A.K. Szakal, and G.F. Burton. 1995. Follicular dendritic cells and human immunodeficiency virus infectivity. *Nature.* 377:740–744.
7. Haase, A.T., K. Henry, M. Zupancic, G. Sedgewick, R.A. Faust, H. Melroe, W. Cavert, K. Gebhard, K. Staskus, Z.Q. Zhang, et al. 1996. Quantitative image analysis of HIV-1 infection in lymphoid tissue. *Science.* 274:985–989.
8. Burton, G.F., A. Masuda, S.L. Heath, B.A. Smith, J.G. Tew, and A.K. Szakal. 1997. Follicular dendritic cells (FDC) in retroviral infection: host/pathogen perspective. *Immunol. Rev.* 156:185–197.
9. MacLennan, I.C.M. 1994. Germinal centers. *Annu. Rev. Immunol.* 12:117–139.
10. Kelsoe, G. 1996. *In situ* studies of the germinal center reaction. *Adv. Immunol.* 60:267–288.
11. Rajewsky, K. 1996. Clonal selection and learning in the antibody system. *Nature.* 381:751–758.
12. Kunkl, A., and G.G.B. Klaus. 1981. The generation of memory cells. I. Immunization with antigen-antibody complexes accelerates the development of B-memory cells, the formation of germinal centres and the maturation of antibody affinity in the secondary response. *Immunology.* 43:371–378.
13. Lindhout, E., G. Koopman, S.T. Pals, and C. de Groot. 1997. Triple check for antigen specificity of B cells during germinal center reactions. *Immunol. Today.* 18:573–577.
14. Androlewicz, M.J., J.L. Browning, and C.F. Ware. 1992. Lymphotoxin is expressed as a heteromeric complex with a distinct 33-kDa glycoprotein on the surface of an activated human T cell hybridoma. *J. Biol. Chem.* 267:2542–2547.
15. Browning, J.L., A. Ngam-ek, P. Lawton, J. DeMarinis, R. Tizard, E.P. Chow, C. Hession, B. O'Brine-Greco, S.F. Foley, and C.F. Ware. 1993. Lymphotoxin β , a novel member of the TNF family that forms a heteromeric complex with lymphotoxin on the cell surface. *Cell.* 72:847–856.
16. Paul, N.L., and N.H. Ruddle. 1988. Lymphotoxin. *Annu. Rev. Immunol.* 6:407–438.
17. Ware, C.F., T.L. VanArsdale, P.D. Crowe, and J.L. Browning. 1995. The ligands and receptors of the lymphotoxin system. *Curr. Top. Microbiol. Immunol.* 198:175–218.
18. Hochman, P.S., G.R. Majeau, F. Mackay, and J.L. Browning. 1996. Proinflammatory responses are efficiently induced by homotrimeric but not heterotrimeric lymphotoxin ligands. *J. Inflamm.* 46:220–234.
19. Browning, J.L., K. Miatkowski, I. Sizing, D. Griffiths, M. Zafari, C.D. Benjamin, W. Meier, and F. Mackay. 1996. Signaling through the lymphotoxin β receptor induces the death of some adenocarcinoma tumor lines. *J. Exp. Med.* 183: 867–878.
20. MacKay, F., P.R. Bourdon, D.A. Griffiths, P. Lawton, M. Zafari, I.D. Sizing, K. Miatkowski, A. Ngam-ek, C.D. Benjamin, C. Hession, et al. 1997. Cytotoxic activities of recombinant soluble murine lymphotoxin- α and lymphotoxin- $\alpha\beta$ complexes. *J. Immunol.* 159:3299–3310.
21. Degli-Esposti, M.A., T. Davis-Smith, W.S. Din, P.J. Smolak, R.G. Goodwin, and C.A. Smith. 1997. Activation of the lymphotoxin β receptor by cross-linking induces chemokine production and growth arrest in A375 melanoma cells. *J. Immunol.* 158:1756–1762.
22. De Togni, P., J. Goellner, N.H. Ruddle, P.R. Streeter, A. Fick, S. Mariathasan, S.C. Smith, R. Carlson, L.P. Shornick, J. Strauss-Schoenberger, et al. 1994. Abnormal development of peripheral lymphoid organs in mice deficient in lymphotoxin. *Science.* 264:703–707.
23. Banks, T.A., B.T. Rouse, M.K. Kerley, P.J. Blair, V.L. Godfrey, N.A. Kuklin, D.M. Bouley, J. Thomas, S. Kanangat, and M.L. Mucenski. 1995. Lymphotoxin- α -deficient mice: effects on secondary lymphoid organ development and humoral immune responsiveness. *J. Immunol.* 155:1685–1693.
24. Matsumoto, M., S.F. Lo, C.J.L. Carruthers, J. Min, S. Mariathasan, G. Huang, D.R. Plas, S.M. Martin, R.S. Geha, M.H. Nahm, and D.D. Chaplin. 1996. Affinity maturation without germinal centers in lymphotoxin- α -deficient mice. *Nature.* 382:462–466.
25. Matsumoto, M., S. Mariathasan, M.H. Nahm, F. Baranyay, J.J. Peschon, and D.D. Chaplin. 1996. Role of lymphotoxin and the type I TNF receptor in the formation of germinal centers. *Science.* 271:1289–1291.
26. Koni, P.A., R. Sacca, P. Lawton, J.L. Browning, N.H. Ruddle, and R.A. Flavell. 1997. Distinct roles in lymphoid organogenesis for lymphotoxins α and β revealed in lymphotoxin β -deficient mice. *Immunity.* 6:491–500.
27. Alimzhanov, M.B., D.V. Kuprash, M.H. Kosco-Vilbois, A. Luz, R.L. Turetskaya, A. Tarakhovskiy, K. Rajewsky, S.A. Nedospasov, and K. Pfeffer. 1997. Abnormal development of secondary lymphoid tissues in lymphotoxin β -deficient mice. *Proc. Natl. Acad. Sci. USA.* 94:9302–9307.
28. Fütterer, A., K. Mink, A. Luz, M.H. Kosco-Vilbois, and K. Pfeffer. 1998. The lymphotoxin β receptor controls organogenesis and affinity maturation in peripheral lymphoid tissues. *Immunity.* 9:59–70.
29. Alexopoulou, L., M. Pasparakis, and G. Kollias. 1998. Complementation of lymphotoxin α knockout mice with tumor necrosis factor-expressing transgenes rectifies defective splenic structure and function. *J. Exp. Med.* 188:745–754.
30. Koni, P.A., and R.A. Flavell. 1998. A role for tumor necrosis factor receptor type 1 in gut-associated lymphoid tissue development: genetic evidence of synergism with lymphotoxin β . *J. Exp. Med.* 187:1977–1983.
31. Grouard, G., I. Durand, L. Filgueira, L. Banchereau, and Y.-J. Liu. 1996. Dendritic cells capable of stimulating T cells in germinal centers. *Nature.* 384:364–367.
32. Kroese, F.G.M., A.S. Wubbena, and P. Nieuwenhuis. 1986. Germinal centre formation and follicular antigen trapping in the spleen of lethally X-irradiated and reconstituted rats. *Immunology.* 57:99–104.
33. MacKay, F., and J.L. Browning. 1998. Turning off follicular dendritic cells. *Nature.* 395:26–27.
34. Kato, J., N. Motoyama, I. Taniuchi, H. Takeshita, M. Toyoda, K. Masuda, and T. Watanabe. 1998. Affinity maturation in Lyn kinase-deficient mice with defective germinal

- center formation. *J. Immunol.* 160:4788–4795.
35. Xu, J., T.M. Foy, J.D. Laman, E.A. Elliott, J.J. Dunn, T.J. Waldschmidt, J. Elsemore, R.J. Noelle, and R.A. Flavell. 1994. Mice deficient for the CD40 ligand. *Immunity.* 1:423–431.
 36. Kelly, B.S., J.G. Levy, and L. Sikora. 1979. The use of enzyme-linked immunosorbent assay (ELISA) for the detection and quantification of specific antibody from cell cultures. *Immunology.* 37:45–52.
 37. Rose, M.L., M.S.C. Birbeck, V.J. Wallis, J.A. Forrester, and A.J.S. Davies. 1980. Peanut lectin binding properties of germinal centers of mouse lymphoid tissue. *Nature.* 284:364–366.
 38. Hardy, R.R., K. Hayakawa, D.R. Parks, L.A. Herzenberg, and L.A. Herzenberg. 1984. Murine B cell differentiation lineages. *J. Exp. Med.* 159:1169–1188.
 39. Lalor, P.A., G.J.V. Nossal, R.D. Sanderson, and M.G. McHeyzer-Williams. 1992. Functional and molecular characterization of single, (4-hydroxy-3-nitrophenyl)acetyl (NP)-specific, IgG₁⁺ B cells from antibody-secreting and memory B cell pathways in C57BL/6 immune response to NP. *Eur. J. Immunol.* 22:3001–3011.
 40. Kimoto, H., H. Nagaoka, Y. Adachi, T. Mizuochi, T. Azuma, T. Yagi, T. Sata, S. Yonehara, Y. Tsunetsugu-Yokota, M. Taniguchi, and T. Takemori. 1997. Accumulation of somatic hypermutation and antigen-driven selection in rapidly-cycling surface Ig⁺ germinal center (GC) B cells which occupy GC at a high frequency during primary anti-hapten response in mice. *Eur. J. Immunol.* 27:268–279.
 41. Ahearn, J.M., M.B. Fischer, D. Croix, S. Goerg, M. Ma, J. Xia, X. Zhou, R.G. Howard, T.L. Rothstein, and M.C. Carroll. 1996. Disruption of the *Cr2* locus results in a reduction in B-1a cells and in an impaired B cell response to T-dependent antigen. *Immunity.* 4:251–262.
 42. Molina, H., V.M. Holars, B. Li, Y.-F. Fang, S. Mariathasan, J. Goellner, J. Strauss-Schoenberger, R.W. Karr, and D.D. Chaplin. 1996. Markedly impaired humoral response in mice deficient in complement receptors 1 and 2. *Proc. Natl. Acad. Sci. USA.* 93:3357–3361.
 43. Maeda, K., G.F. Burton, D.A. Padgett, D.H. Conrad, T.F. Huff, A. Masuda, A. Szakal, and J.G. Tew. 1992. Murine follicular dendritic cells (FDC) and low affinity Fc-receptors for IgE (FcεRII). *J. Immunol.* 148:2340–2347.
 44. Han, S., S.R. Dillon, B. Zheng, M. Shimoda, M.S. Schlissel, and G. Kelsoe. 1997. V(D)J recombinase activity in a subset of germinal center B lymphocytes. *Science.* 278:301–305.
 45. Takahashi, Y., P.R. Dutta, D.M. Cerasoli, and G. Kelsoe. 1998. In situ studies of the primary immune response to (4-hydroxy-3-nitrophenyl)acetyl. V. Affinity maturation developments in two stages of clonal selection. *J. Exp. Med.* 187:885–895.
 46. Jacob, J., R. Kassir, and G. Kelsoe. 1991. In situ studies of the primary immune response to (4-hydroxy-3-nitrophenyl) acetyl. I. The architecture and dynamics of responding cell populations. *J. Exp. Med.* 173:1165–1175.
 47. Jacob, J., and G. Kelsoe. 1992. In situ studies of the primary immune response to (4-hydroxy-3-nitrophenyl)acetyl. II. A common clonal origin for periarteriolar lymphoid sheath-associated foci and germinal centers. *J. Exp. Med.* 176:679–687.
 48. Jacob, J., J. Przylepa, C. Miller, and G. Kelsoe. 1993. In situ studies of the primary immune response to (4-hydroxy-3-nitrophenyl)acetyl. III. The kinetics of V region mutation and selection in germinal center B cells. *J. Exp. Med.* 178:1293–1307.
 49. Jack, R.S., T. Imanishi-Kari, and K. Rajewsky. 1977. Idiotypic analysis of the response of C57BL/6 mice to the (4-hydroxy-3-nitrophenyl)acetyl group. *Eur. J. Immunol.* 8:559–565.
 50. Makela, O., and K. Karjalainen. 1977. Inherited immunoglobulin idiotypes of the mouse. *Immunol. Rev.* 34:119–138.
 51. Reth, M., T. Imanishi-Kari, and K. Rajewsky. 1979. Analysis of the repertoire of anti-NP antibodies in C57BL/6 mice by cell fusion. II. Characterization of idiotopes by monoclonal anti-idiotope antibodies. *Eur. J. Immunol.* 9:1004–1013.
 52. Cumano, A., and K. Rajewsky. 1985. Structure of primary anti-(4-hydroxy-3-nitrophenyl)acetyl (NP) antibodies in normal and idiotypically suppressed C57BL/6 mice. *Eur. J. Immunol.* 15:512–520.
 53. Matsumoto, M., Y.-X. Fu, H. Molina, G. Huang, J. Kim, D.A. Thomas, M.H. Nahm, and D.D. Chaplin. 1997. Distinct roles of lymphotoxin α and type I tumor necrosis factor (TNF) receptor in the establishment of follicular dendritic cells from non-bone marrow-derived cells. *J. Exp. Med.* 186:1997–2004.
 54. Maeda, K., M. Matsuda, and Y. Imai. 1995. Follicular dendritic cells: structure as related to function. *Curr. Top. Microbiol. Immunol.* 201:119–139.
 55. Kapasi, Z.F., D. Qin, W.G. Kerr, M.H. Kosco-Vilbois, L.D. Shultz, J.G. Tew, and A.K. Szakal. 1998. Follicular dendritic cell (FDC) precursors in primary lymphoid tissues. *J. Immunol.* 160:1078–1084.
 56. Kosco-Vilbois, M.H., H. Zentgraf, J. Gerdes, and J.-Y. Bonnefoy. 1997. To 'B' or not to 'B' a germinal center? *Immunol. Today.* 18:225–230.
 57. Weiss, U., R. Zoebelin, and K. Rajewsky. 1992. Accumulation of somatic mutants in the B cell compartment after primary immunization with a T cell-dependent antigen. *Eur. J. Immunol.* 22:511–517.
 58. McHeyzer-Williams, M.G., M.J. McLean, P.A. Lalor, and G.J.V. Nossal. 1993. Antigen-driven B cell differentiation in vivo. *J. Exp. Med.* 178:295–307.
 59. Casson, L.P., and T. Manser. 1995. Random mutagenesis of two complementarity determining region amino acids yields an unexpectedly high frequency of antibodies with increased affinity for both cognate antigen and autoantigen. *J. Exp. Med.* 182:743–750.
 60. Bothwell, A.L.M., M. Paskind, M. Reth, T. Imanishi-Kari, K. Rajewsky, and D. Baltimore. 1981. Heavy chain variable region contribution to the NP^b family of antibodies: somatic mutation evident in a γ2a variable region. *Cell.* 24:625–637.
 61. Allen, D., T. Simon, F. Sablitzky, K. Rajewsky, and A. Cumano. 1988. Antibody engineering for the analysis of affinity maturation of an anti-hapten response. *EMBO (Eur. Mol. Biol. Organ.) J.* 7:1995–2000.
 62. Gray, D., and T. Leanderson. 1990. Expansion, selection and maintenance of memory B-cell clones. *Curr. Top. Microbiol. Immunol.* 159:1–17.
 63. MacLennan, I.C.M., Y.J. Liu, S. Oldfield, J. Zhang, and P.J.L. Lane. 1990. The evolution of B-cell clones. *Curr. Top. Microbiol. Immunol.* 159:37–63.
 64. Liu, Y.-J., J. Zhang, P.J.L. Lane, E.Y.-T. Chan, and I.C.M. MacLennan. 1991. Sites of specific B cell activation in primary and secondary responses to T cell-dependent and T cell-independent antigens. *Eur. J. Immunol.* 21:2951–2962.
 65. MacLennan, I.C.M., A. Gulbranson-Judge, K.-M. Toellner, M. Casamayor-Palleja, E. Chan, D.M.-Y. Sze, S.A. Luther, and H.A. Orbea. 1997. The changing preference of T and B cells for partners as T-dependent antibody responses develop. *Immunol. Rev.* 156:53–66.
 66. Liu, Y.-J. 1997. Sites of B lymphocyte selection, activation, and tolerance in spleen. *J. Exp. Med.* 186:625–629.